# Supplemental Materials

***Molecular Biology of the Cell***

Daou et al.

## SUPPLEMENTAL TABLE LEGENDS:

**TABLE S1:** Proteins binding to the FH2 domain of mDia1. Sheet 1: Proteins present in the EGFP-FH2 pulldowns were identified by mass spectrometry. Proteins increased more than two-fold in the EGFP-FH2 pulldown versus control (EGFP) with a $p<0.05$ are shown. The number of peptide identified, score, fold increase and ANOVA are indicated. Sheet 2: Fold change and ANOVA of protein abundance in EGFP-WIK2 relative to EGFP-FH2 pulldowns are shown.

**TABLE S2:** Proteins binding to the FH2 domains of mDia1, mDia2 and mDia3. Proteins present in the EGFP-mDia1-FH2, EGFP-mDia2-FH2 and EGFP-mDia3-FH2 pulldowns were identified by mass spectrometry. Proteins strongly increased in the EGFP-FH2 pulldowns relative to EGFP control pulldown and found in at least 2 out of 3 independent experiments are shown. Experiment 1, 2 and 3 were performed from 2.5,5 and 7 mg protein lysates, respectively. Total number of identified peptide sequences is shown.

## SUPPLEMENTAL FIGURE LEGENDS:

**FIGURE S1:** Validation of siRNA efficiency. SKBr3 cells were transfected with the indicated siRNA for 48 h, before cell lysates collection and Western blotting analysis with the indicated antibody. Tubulin served as loading control. For mDia formins, expression of ectopically expressed EGFP-mDia cDNAs is also shown.

**FIGURE S2:** Concomitant inhibition of mDia1, mDia2 and mDia3 had no major impact on actin cytoskeleton organization. SKBr3 cells were transfected with control (Ctrl) siRNA or siRNAs against mDia1, mDia2 and mDia3, together with an EGFP-actin construct. Actin-EGFP expressing cells were visualized by time-lapse microscopy 20 min after addition of HRG. (**A**) The number of microspikes (filopodia-like structures) in each cell was evaluated and normalized to the width of the protrusion; 20 cells were counted per condition in three independent experiments. Mean +/- s.e.m. is shown. (**B**) The width of the cortical actin network (shown on the right panel) was evaluated. 15 cells were counted per condition in three independent experiments; mean +/- s.e.m. is shown. (C) Cells expressing control (Ctrl) or mDia1, mDia2 and mDia3 siRNAs were treated with 5 nM HRG for 20 min and fixed, before F-actin labeling with fluorescent phalloidin. No significant differences were seen in stress fiber (arrows) formation.

**FIGURE S3**: mDia1, mDia2 and mDia3 are required for ErbB2-induced microtubule capture. Cells were transfected with the indicated siRNA and cDNA coding for wild-type mDia1, mDia2 or mDia3. The siRNA against mDia1 and mDia3 used in this experiment targets a non-coding sequences (in the 3' and 5'UTR, respectively). The siRNA against mDia2 targets a sequence which matches the human, but not the mouse sequence. Mouse mDia2 is used for rescue. The percentage of cells with peripheral microtubules was evaluated as described in Figure 1. Mean +/- s.e.m. is shown; * $p<0.01$. Re-expression an mDia compensates siRNA-mediated inhibition of the corresponding mDia to allow cortical microtubule formation.

**FIGURE S4**: Overexpression of a single mDia is not sufficient for microtubule capture. (**A**) Cells were transfected with the indicated mDia siRNA cDNA for active mDia formins (ΔNmDia). EGFP- or mCherry-tubulin-expressing cells were visualized by time-lapse microscopy and the percentage of cells with peripheral microtubules was evaluated 20 min after addition of HRG as described in Figure 1. Mean +/- s.e.m. is shown; * $p<0.01$. (**B**) Still images of EGFP-or mCherry-tubulin expressing cells are shown. Insets: zooms showing the presence or absence of microtubules in cell protrusions.

**FIGURE S5**: Characterization of mDia molecular mechanisms of action. (**A**) Cells were transfected with the indicated mDia siRNA and with a cDNA coding for a membrane-targeted form of ACF7 (ACF-CCKVL) or mDia mutants. mCherry-tubulin expressing cells were visualized by time-lapse microscopy 20 min after addition of HRG. Still images corresponding to the experiment quantified in Figure 3A are shown. Insets: zooms showing the presence or absence of microtubules in cell protrusions. The expression of ACF7-CCKVL compensates the loss of mDia1, but not of mDia2 or mDia3. (**B**) Cells were transfected with control (Ctrl) or mDia1 siRNA and with cDNA for the indicated FH2 constructs. EGFP-tubulin expressing cells were visualized by time-lapse microscopy 20 min after addition of HRG. Still images corresponding to the experiment quantified in Figure 3B are shown. The FH2 of mDia1, mDia2 and mDia3 is sufficient to restore microtubule capture.

**FIGURE S6**: Determination of mDia1 functional domain for microtubule capture. (**A**) Schematic showing the constructs used in the experiments: $mDia1_{543-1192}$ (ΔNmDia1), $mDia_{1682-1192}$ (ΔΔN mDia1) and $mDia1_{752-1192}$ (FH2). (**B**) Cells were transfected with control (Ctrl) or mDia1 siRNA and with the indicated cDNA construct. EGFP-tubulin-expressing cells were visualized by time-lapse microscopy and the percentage of cells with peripheral microtubules was evaluated 20 min after addition of HRG. The percentage of cells with peripheral microtubules was evaluated as described in Figure 1. Mean +/- s.e.m. is shown; * $p<0.01$. The expression of the FH2 domain is sufficient to restore microtubule capture. (**C**) mDia1 mutant constructs are expressed at levels similar to the wt construct (related to Figure 3D).

**FIGURE S7:** Proteomic analysis of the FH2 mutants (**A**) Schematic description of the FH2-WIK2 and FH2-WIK3 mutant constructs. The W767A, I845A and K994/999A mutations were introduced in the FH2 domain of mDia1 to produce the FH2WIK2 mutant. An additional K989A mutation was introduces in FH2-WIK2 to produce FH2-WIK3 (**B**) Concomitant introduction of W767A, I845A and K994/999A mutations does not affect microtubule capture. Cells were transfected with control (Ctrl) or mDia1 siRNA and with cDNA coding for the FH2 or FH2-WIK2, as indicated. EGFP-tubulin expressing cells were visualized by time-lapse microscopy. The percentage of cells with peripheral microtubules was evaluated as described in Figure 1. Mean +/- s.e.m. is shown; * $p<0.01$. (**D-E**) Volcano plot showing proteins whose interaction is diminished in the FH2-WIK2 mutant (**E**) or FH2-WIK3 mutant (**F**) relative to wild type FH2. Only proteins that showed significant binding to FH2 in Figure 4A (fold change>2) were included in the analysis. No further protein interaction was lost by introduction of the K989A mutation into WIK2.

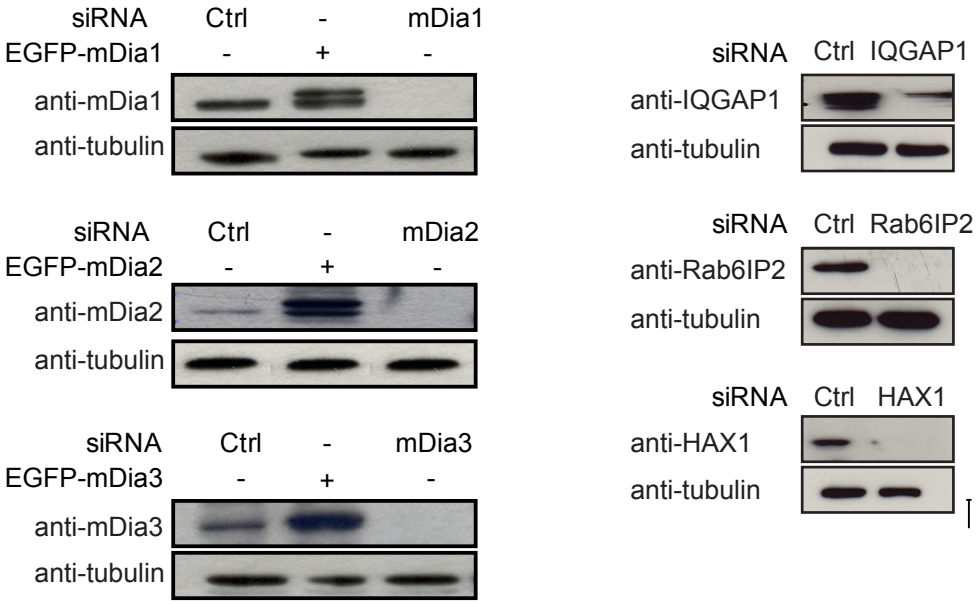


**FIGURE S1:** Validation of siRNA efficiency. SKBr3 cells were transfected with the indicated siRNA for 48 h, before cell lysates collection and Western blotting analysis with the indicated antibody. Tubulin served as loading control. For mDia formins, expression of ectopically expressed EGFP-mDia cDNAs is also shown.

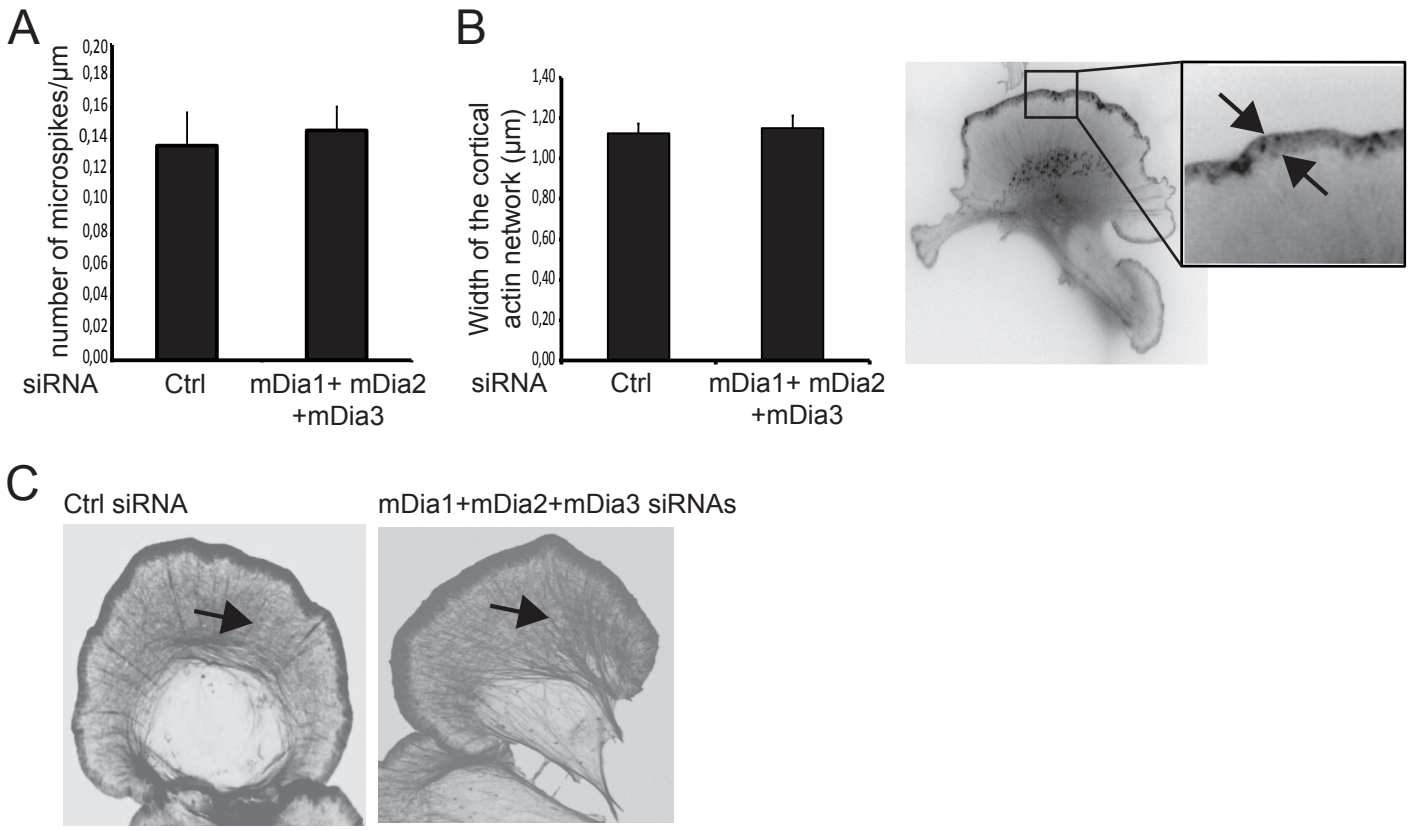


**FIGURE S2:** Concomitant inhibition of mDia1, mDia2 and mDia3 had no major impact on actin cytoskeleton organization. SKBr3 cells were transfected with control (Ctrl) siRNA or siRNAs against mDia1, mDia2 and mDia3, together with an EGFP-actin construct. Actin-EGFP expressing cells were visualized by time-lapse microscopy 20 min after addition of HRG. (**A**) The number of microspikes (filopodia-like structures) in each cell was evaluated and normalized to the width of the protrusion; 20 cells were counted per condition in three independent experiments. Mean +/- s.e.m. is shown. (**B**) The width of the cortical actin network (shown on the right panel) was evaluated. 15 cells were counted per condition in three independent experiments; mean +/- s.e.m. is shown. (C) Cells expressing control (Ctrl) or mDia1, mDia2 and mDia3 siRNAs were treated with 5 nM HRG for 20 min and fixed, before F-actin labeling with fluorescent phalloidin. No significant differences were seen in stress fiber (arrows) formation.

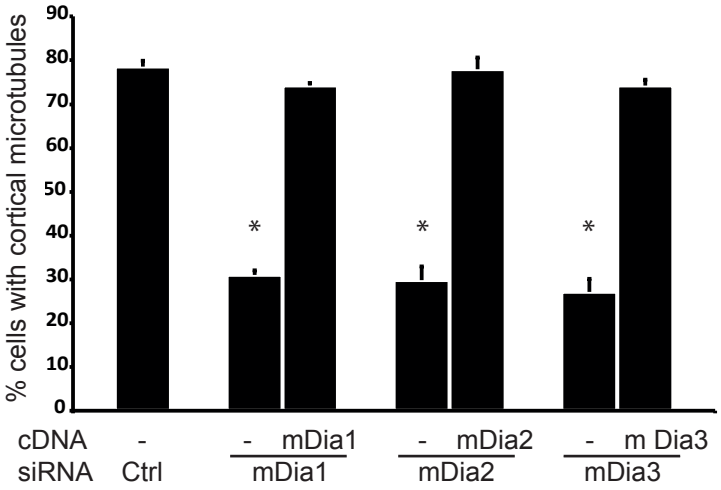


**FIGURE S3**: mDia1, mDia2 and mDia3 are required for ErbB2-induced microtubule capture. Cells were transfected with the indicated siRNA and cDNA coding for wild-type mDia1, mDia2 or mDia3. The siRNA against mDia1 and mDia3 used in this experiment targets a non-coding sequences (in the 3' and 5'UTR, respectively). The siRNA against mDia2 targets a sequence which matches the human, but not the mouse sequence. Mouse mDia2 is used for rescue. The percentage of cells with peripheral microtubules was evaluated as described in Figure 1. Mean +/- s.e.m. is shown; * $p<0.01$. Re-expression an mDia compensates siRNA-mediated inhibition of the corresponding mDia to allow cortical microtubule formation.

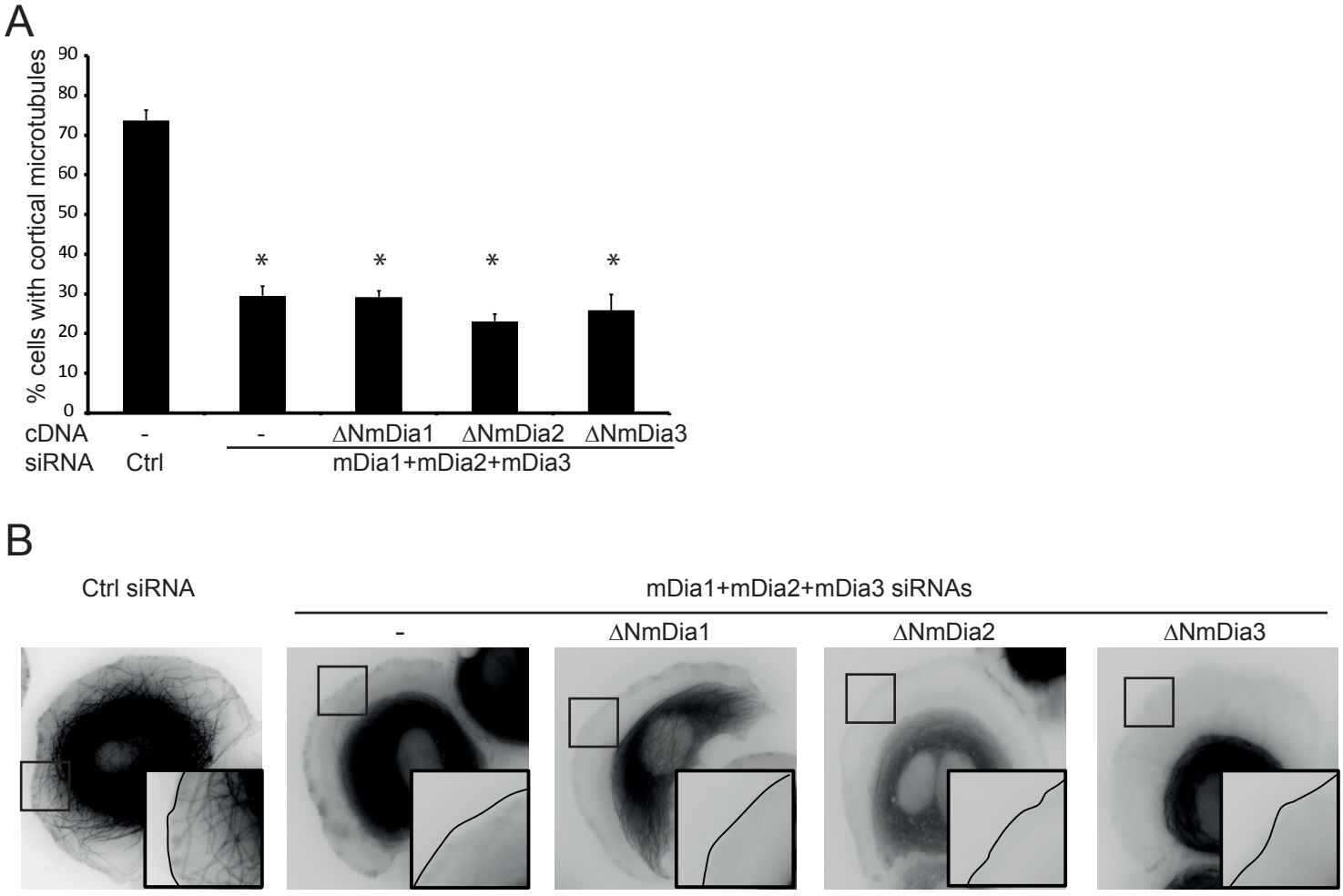


**FIGURE S4**: Overexpression of a single mDia is not sufficient for microtubule capture. (**A**) Cells were transfected with the indicated mDia siRNA cDNA for active mDia formins (ΔNmDia). EGFP- or mCherry-tubulin-expressing cells were visualized by time-lapse microscopy and the percentage of cells with peripheral microtubules was evaluated 20 min after addition of HRG as described in Figure 1. Mean +/- s.e.m. is shown; * $p<0.01$. (**B**) Still images of EGFP-or mCherry-tubulin expressing cells are shown. Insets: zooms showing the presence or absence of microtubules in cell protrusions.

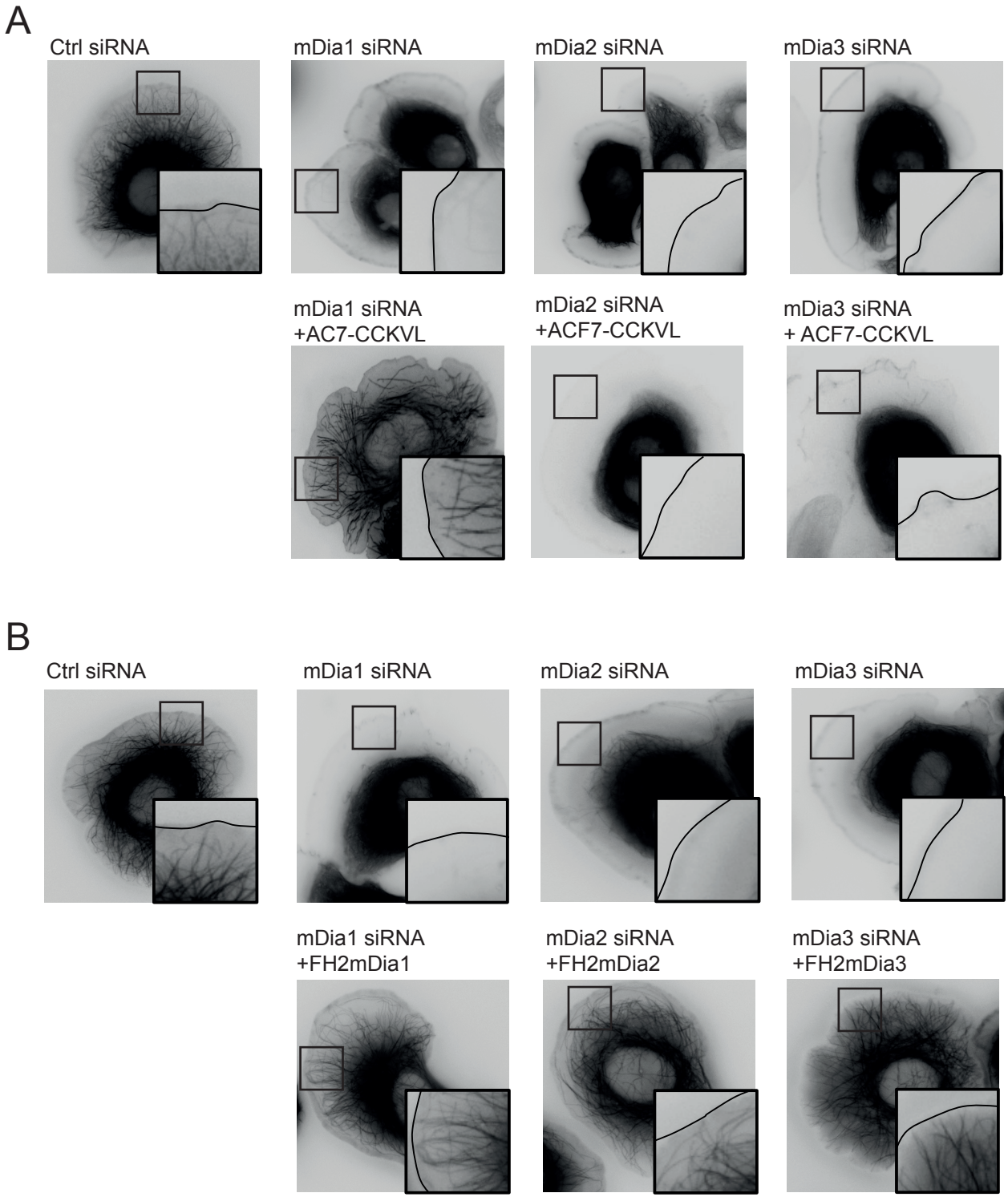


**FIGURE S5**: Characterization of mDia molecular mechanisms of action. (**A**) Cells were transfected with the indicated mDia siRNA and with a cDNA coding for a membrane-targeted form of ACF7 (ACF-CCKVL) or mDia mutants. mCherry-tubulin expressing cells were visualized by time-lapse microscopy 20 min after addition of HRG. Still images corresponding to the experiment quantified in Figure 3A are shown. Insets: zooms showing the presence or absence of microtubules in cell protrusions. The expression of ACF7-CCKVL compensates the loss of mDia1, but not of mDia2 or mDia3. (**B**) Cells were transfected with control (Ctrl) or mDia1 siRNA and with cDNA for the indicated FH2 constructs. EGFP-tubulin expressing cells were visualized by time-lapse microscopy 20 min after addition of HRG. Still images corresponding to the experiment quantified in Figure 3B are shown. The FH2 of mDia1, mDia2 and mDia3 is sufficient to restore microtubule capture.

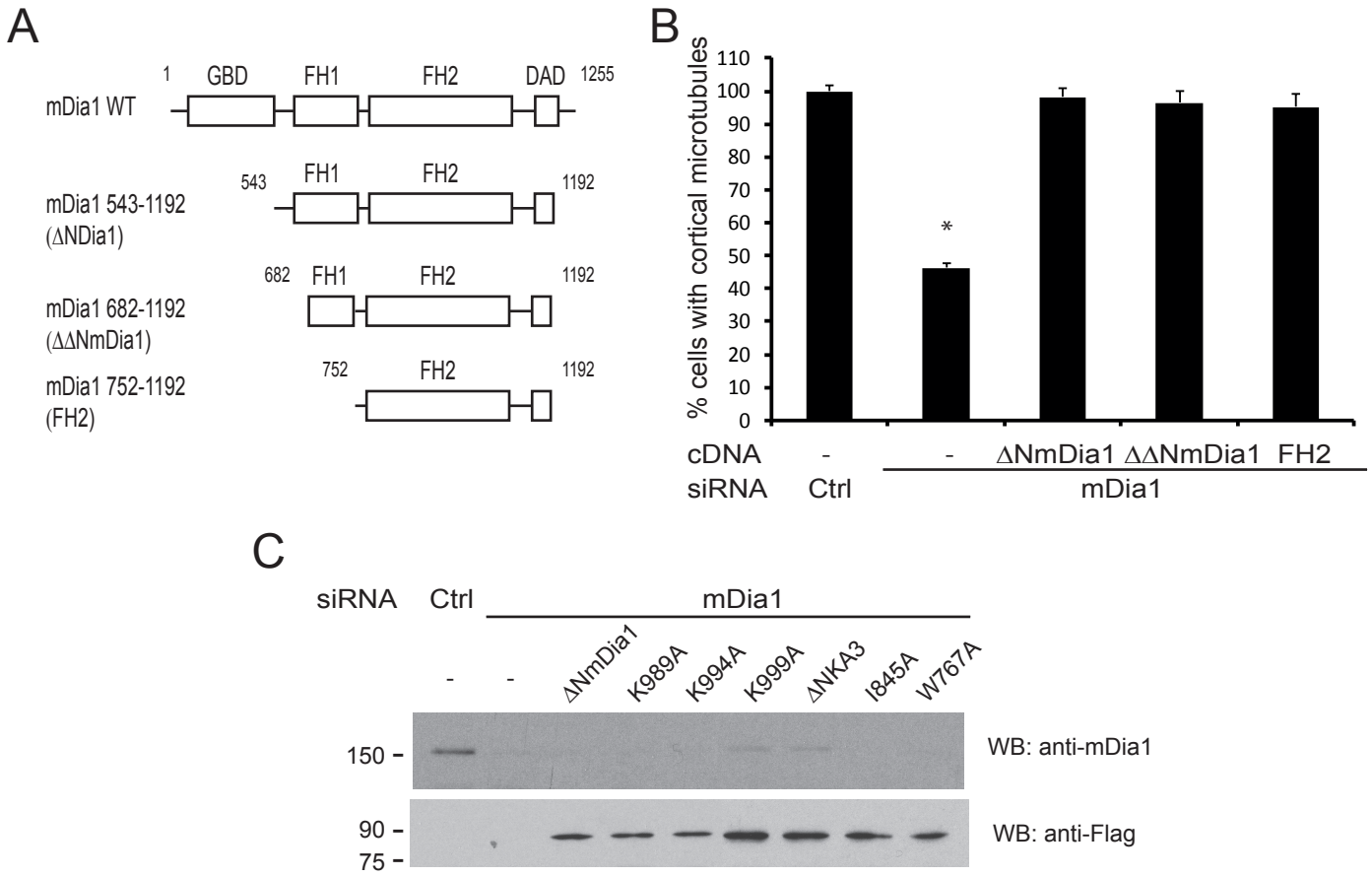


**FIGURE S6**: Determination of mDia1 functional domain for microtubule capture. (**A**) Schematic showing the constructs used in the experiments: $mDia1_{543-1192}$ (ΔNmDia1), $mDia_{1682-1192}$ (ΔΔN mDia1) and $mDia1_{752-1192}$ (FH2). (**B**) Cells were transfected with control (Ctrl) or mDia1 siRNA and with the indicated cDNA construct. EGFP-tubulin-expressing cells were visualized by time-lapse microscopy and the percentage of cells with peripheral microtubules was evaluated 20 min after addition of HRG. The percentage of cells with peripheral microtubules was evaluated as described in Figure 1. Mean +/- s.e.m. is shown; * $p<0.01$. The expression of the FH2 domain is sufficient to restore microtubule capture. (**C**) mDia1 mutant constructs are expressed at levels similar to the wt construct (related to Figure 3D).

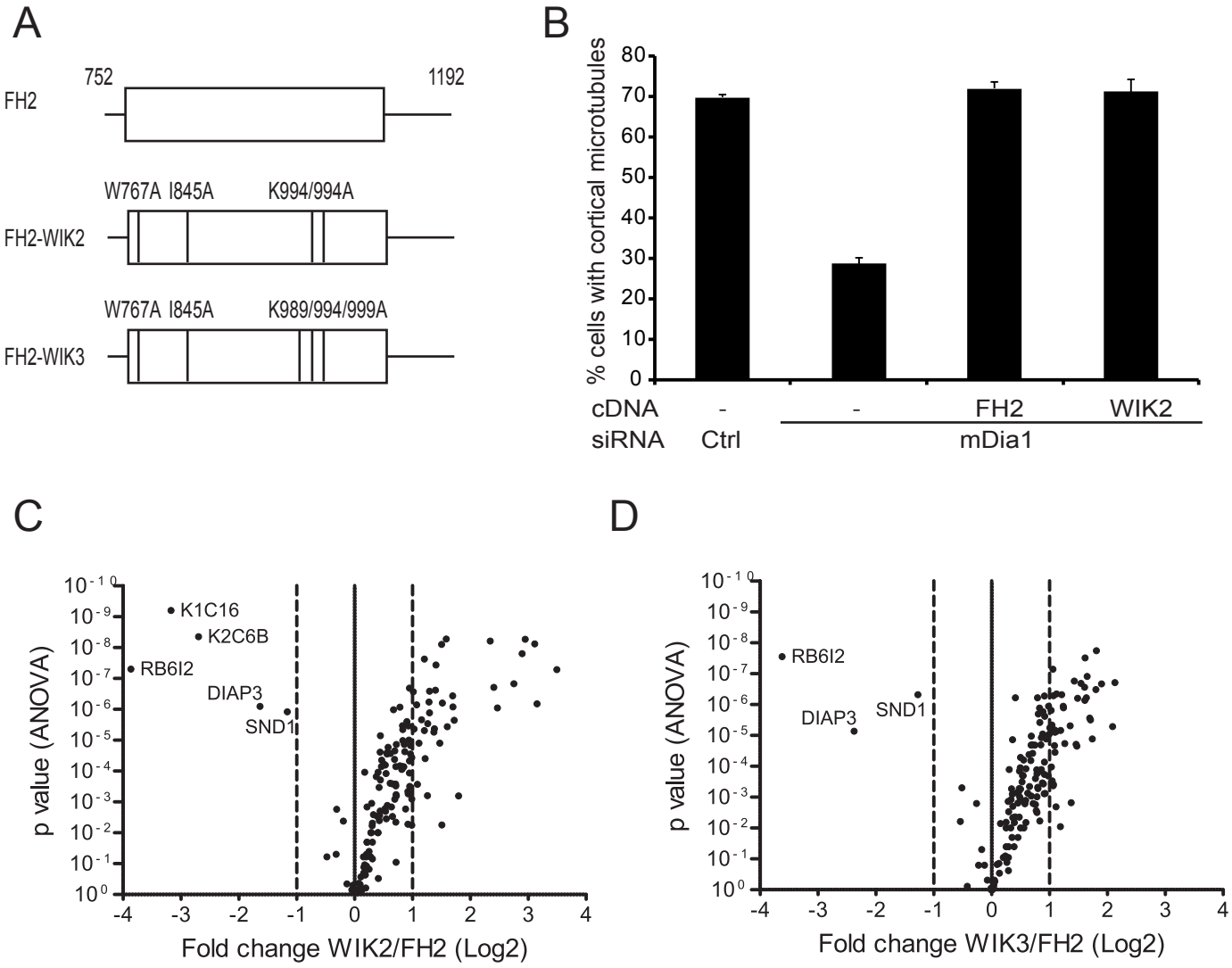


**FIGURE S7:** Proteomic analysis of the FH2 mutants (**A**) Schematic description of the FH2-WIK2 and FH2-WIK3 mutant constructs. The W767A, I845A and K994/999A mutations were introduced in the FH2 domain of mDia1 to produce the FH2WIK2 mutant. An additional K989A mutation was introduces in FH2-WIK2 to produce FH2-WIK3 (**B**) Concomitant introduction of W767A, I845A and K994/999A mutations does not affect microtubule capture. Cells were transfected with control (Ctrl) or mDia1 siRNA and with cDNA coding for the FH2 or FH2-WIK2, as indicated. EGFP-tubulin expressing cells were visualized by time-lapse microscopy. The percentage of cells with peripheral microtubules was evaluated as described in Figure 1. Mean +/- s.e.m. is shown; * $p<0.01$. (**D-E**) Volcano plot showing proteins whose interaction is diminished in the FH2-WIK2 mutant (**E**) or FH2-WIK3 mutant (**F**) relative to wild type FH2. Only proteins that showed significant binding to FH2 in Figure 4A (fold change>2) were included in the analysis. No further protein interaction was lost by introduction of the K989A mutation into WIK2.